Available online at www.sciencedirect.com
ScienceDirect
Journal of Nuclear Materials 373 (2008) 309–318
journal of nuclear materials
www.elsevier.com/locate/jnucmat

Development of CAP process for fabrication of ThO_2–UO_2 fuels Part II: Characterization and property evaluation

T.R.G. Kutty [a,*], R.V. Kulkarni [b], P. Sengupta [c], K.B. Khan [a], K. Bhanumurthy [c], A.K. Sengupta [a], J.P. Panakkal [d], Arun Kumar [a], H.S. Kamath [e]

[a] Radiometallurgy Division, Bhabha Atomic Research Centre, Trombay, Mumbai 400 085, India
[b] Post Irradiation Examination Division, Bhabha Atomic Research Centre, Trombay, Mumbai 400 085, India
[c] Materials Science Division, Bhabha Atomic Research Centre, Trombay, Mumbai 400 085, India
[d] Advanced Fuel Fabrication Facility, Tarapur, India
[e] Nuclear Fuels Group, Bhabha Atomic Research Centre, Trombay, Mumbai 400 085, India

Received 10 October 2006; accepted 22 June 2007

Abstract

Coated agglomerate pelletization (CAP) process is being developed for the fabrication of ThO_2–UO_2 mixed oxide fuel pellets. The procedure for the fabrication of ThO_2–4%UO_2 and ThO_2–20%UO_2 pellets by this process has been described in detail in part I of this series of papers. The present part II deals with the characterization of the above pellets by optical microscopy, scanning electron microscopy (SEM) and electron probe microanalysis (EPMA). The microstructure of the ThO_2–4%UO_2 and ThO_2–20%UO_2 pellets showed a duplex grain structure. Thermal expansion and thermal conductivity were measured in the temperature range from room temperature to 1500 °C. It was found that the thermal conductivity decreased by the addition of UO_2 to ThO_2 at any temperature. Addition of 20%UO_2 to ThO_2 caused very large decrease in thermal conductivity. The thermal expansion of ThO_2–20%UO_2 pellet was different from that of ThO_2 and ThO_2–4%UO_2, e.g. it increased more rapidly with increasing temperature in the temperature range of 1000–1500 °C.

PACS: 61.72; 65.70; 72.15.E; 83.50.Q

1. Introduction

Fabrication of ThO_2–4%UO_2 and ThO_2–20%UO_2 pellets by a novel technique (CAP process) has been described in detail in part I of this series of papers. This part (part II) deals with the microstructural evaluation and determination of thermophysical properties of the above pellets. The microstructure is important since it is deeply related to the irradiation behaviour. It controls the in-pile fuel behaviour like plasticity, in-pile creep and swelling [1]. The microstructure of the fuel is intimately related to the behavior of the fission gases. The improvement in plasticity and fission gas release can be attained by modifying the microstructures during fabrication [2–6]. The conventional process for nuclear ceramics fabrication consists of a number of stages including calcination, milling, incorporating additives, pressing, drying and densification. Since each of these process steps affects the microstructure of the fuel pellets they must all be understood. It is possible to obtain a wide range of microstructures for ThO_2–UO_2 system if the CAP is chosen. This process can tailor the microstructure for better performance during irradiation.

The behaviour of nuclear fuel during irradiation is largely dependent on its physico-chemical properties and their change with temperature and burn-up [7]. Thermal conductivity is an important parameter to understand the performance of the fuel pins under irradiation [1]. If the thermal conductivity is low, the temperature gradient in the radial

* Corresponding author. Fax: +91 22 2550 5151.
E-mail address: tkutty@barc.gov.in (T.R.G. Kutty).

0022-3115/$ - see front matter © 2007 Elsevier B.V. All rights reserved.
doi:10.1016/j.jnucmat.2007.06.011

direction of the fuel pellet is large causing to give high temperature at the central part of the fuel pin [1,7]. The thermal conductivity of nuclear fuel influences almost all important processes such as fission gas release, swelling, grain growth etc. and limits the linear power [8,9]. The changes in thermal conductivity occurs during irradiation by the formation of fission gas bubbles, build-up of fission products, and by the change of oxygen-to-metal ratio (O/M) [10]. Hence the knowledge of thermal conductivity is needed to evaluate its thermal performance. The coefficient of thermal expansion (CTE) values are needed to calculate stresses occurring in the fuel and cladding on change in temperature. If the thermal expansion varies considerably between the fuel and cladding, stresses will be accumulated during the thermal cycling [11]. This can lead to the deformation of the clad and eventually may result in the breakage of the clad. Hence, precise evaluation of CTE data of the fuel is needed.

This paper deals with characterization of ThO_2–4%UO_2 and ThO_2–20%UO_2 pellets made by CAP process with the help of optical microscopy, XRD, SEM and EPMA. The microstructures are evaluated in terms of grain size, pore size and its distribution and homogeneity of uranium. This paper also describes the evaluation of thermal conductivity and thermal expansion for the mixed oxide pellets of the above compositions at temperatures up to 1500 °C, and discusses the effect of composition, microstructure and O/M ratio on the experimental results.

2. Experimental

2.1. Sample preparation

ThO_2–4%UO_2 and ThO_2–20%UO_2 pellets for this study was prepared by the CAP process as described in part I. The pellets were sintered in air at 1450 °C for 8 h. The sintered pellets were about 12 mm in diameter and around 10 mm in length. Table 1 gives details of the samples studied in this work. For metallography, the sintered pellet was fixed by Araldite and ground using successive grades of emery papers. The final polishing was done using diamond paste. The pellet was removed from the mount by dissolving the mount in acetone and then etched thermally by holding the sample at 1400 °C for 4 h in air. The grain size was determined by the intercept method. The microstructure was then characterized by scanning electron microscopy. The distribution of Th, U and O was determined by X-ray mapping and also by line scans with the help of EPMA. A few ThO_2 pellets were also made using the above technique as control samples under the same conditions.

2.2. Thermal conductivity

The studies were carried out using a Ulvac Sinku-Riko (model TC 3000) thermal diffusivity apparatus. For the thermal diffusivity measurement, the sintered pellet was sliced into discs of about 10 mm diameter and 2 mm thickness using a low speed cut-off wheel. A pulse of laser was projected on to the front surface of the pellet and the temperature rise on the rear side of the pellet was recorded as a transient signal by using an infrared detector. The measurements of the thermal diffusivity were carried out up to 1500 °C in vacuum at a pressure of less than 10^{-5} Pa. At each temperature, measurement was carried out thrice. The average value of these three measurements was used and the experimental uncertainty associated with these measurements was within 5%. The thermal diffusivity (α) was calculated from the following relationship:

$$\alpha = WL^2/\pi t_{1/2}, \tag{1}$$

where $t_{1/2}$ the time required in seconds to reach half of the maximum temperature rise at the rear surface of the sample and L the sample thickness in millimeter. W a dimensionless parameter which is a function of the relative heat loss from the sample during the measurement. The data was corrected for radiation heat losses by the method of Clark and Taylor [12].

The thermal conductivities of ThO_2, ThO_2–4%UO_2 and ThO_2–20%UO_2 pellets were derived from the measured values of thermal diffusivity data determined by laser flash technique by using the relation:

$$\lambda = \alpha\rho C_p, \tag{2}$$

where λ the thermal conductivity, α the thermal diffusivity, ρ the density of the material and C_p its specific heat at constant pressure. The literature values of specific heat were used in this study and specific heat capacity of (Th,U)O_2 was estimated from those of ThO_2 [13] and UO_2 [7] using the Kopp's law.

2.3. Thermal expansion

The thermal expansion of ThO_2, ThO_2–4%UO_2 and ThO_2–20%UO_2 pellets was measured by a Netzsch (model 402E) horizontal dilatometer in Ar atmosphere with a heating rate of 6 K/min. The accuracy of the measurement of

Table 1
Density, pore fraction and O/M ratio of ThO_2, ThO_2–4%UO_2 and ThO_2–20%UO_2 pellets fabricated by CAP process

Sample	O/M ratio	Bulk density g/cm^3	Theoretical density (T.D.)	% T.D.	% Pore fraction
ThO_2	2.00	9.203	10.00	92.03	7.97
ThO_2–4%UO_2	2.01	9.451	10.038	94.15	5.85
ThO_2–20%UO_2	2.07	9.211	10.192	90.37	9.63

change in length was within ±0.1 μm. The coefficient of thermal expansion (CTE) was calculated by a software package attached to the dilatometer. Data correction was made using the standard sample (poco graphite – NIST). The coefficient of thermal expansion (CTE) between two temperatures T_1 and T_2 can be calculated using the relation:

$$\mathrm{CTE}_{(T_1-T_2)} = [(L_2 - L_1)/L_0][1/(T_2 - T_1)], \quad (3)$$

where L_0 the initial length of the specimen at room temperature, L_1 and L_2 are the lengths at temperatures T_1 and T_2, respectively.

3. Results

The XRD data of ThO_2–20%UO_2 showed that it was a single phase compound. Fig. 1 shows the SEM microstructure of the ThO_2–4%UO_2 pellet sintered in air. This pellet is made by coating ThO_2 granules with U_3O_8 powder followed by pressing and sintering in air. On heating, U_3O_8 decomposes to UO_{2+x} and forms a solid solution with ThO_2. The presence of Th and U was noticed at all places in the pellet by the EPMA scan. This shows that the chemical identity of the staring material is lost and U ions have migrated to ThO_2 granules and vice versa. It is true that the identity of the granules is still noticed after sintering. But their chemical composition has been changed. The grains were found to be duplex in nature. The grain size distribution is similar to 'rock in sand' structure. There were packets of fine grains uniformly distributed in the matrix. The average size of these fine grains was 1.7 μm. The grain size of the matrix was around 7–8 μm (Fig. 2). The pore distribution was found to be non-uniform with most of the pores being located on large grained areas. The packets of fine grains were found to be very dense with very little porosity. Fig. 3 shows the microstructure of starting material viz. ThO_2. The microstructure shows that the grain size varies from 2 to 15 μm, with an average value around 5 μm. ThO_2 is a single phase compound and no change in the composition is occurring on sintering. On the other hand, ThO_2–4%UO_2 pellet is produced from ThO_2 granules and

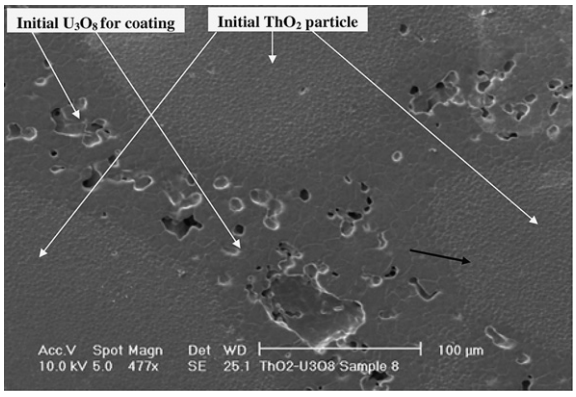

Fig. 1. Microstructure of ThO_2–4%UO_2 pellet showing duplex grain structure. Pellet: sintered in air and etched thermally.

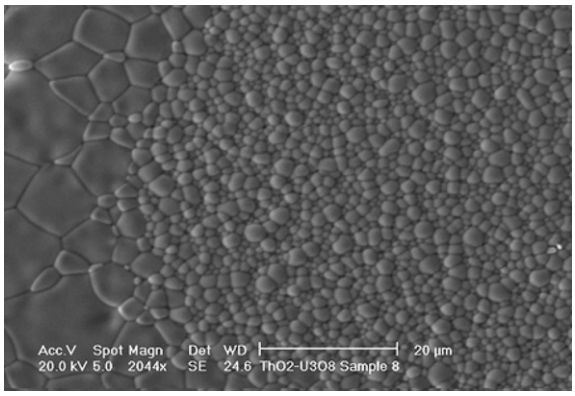

Fig. 2. Microstructure of ThO_2–4%UO_2 pellet showing interface between granules. No pores were detected in the fine grained region. The region shown by a black arrow in Fig. 1 has been magnified and shown here.

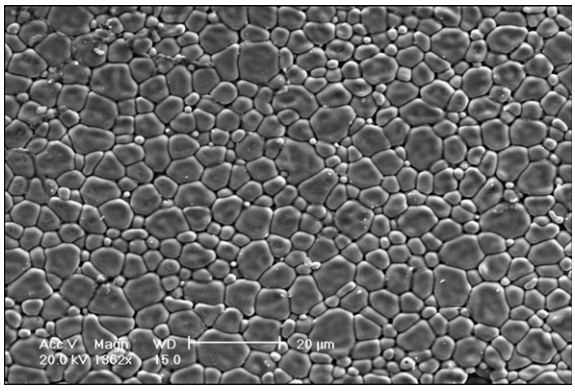

Fig. 3. Microstructure of sintered ThO_2 pellet showing uniform grain structure.

U_3O_8 powder as the starting materials. As mentioned earlier, U_3O_8 decomposes to UO_{2+x} at high temperatures and forms $(Th,U)O_{2+x}$ solid solution. This results in the creation of large amount of defects in this region. Therefore diffusion is enhanced. Since grain growth is a diffusion controlled process, this will lead to larger grain sizes. The initial ThO_2 region becomes $(Th,U)O_2$ after sintering. Since defects are less here, grain growth is retarded and therefore grains are smaller in this region.

The microstructure of ThO_2–20%UO_2 pellet is shown in Fig. 4. The microstructure was found to be highly non-uniform with most of the pores being located on the initial U_3O_8 for coating. It is duplex similar to that of ThO_2–4%UO_2 pellets. A large number of pores exist in large grained region when compared with ThO_2–4%UO_2 pellets. To find out the distribution of Th, U and O in the ThO_2 matrix, a detailed study was carried out by scanning electron beam across the duplex structure by means of EPMA. A typical BSE image is shown in Fig. 5 for ThO_2–4%UO_2 pellet and the corresponding X-ray line scan for Th M_α, U M_α and O K_α are also shown in the same figure. The exact region of this scan is marked in the BSE image (Fig. 5) as A–B. The line scan clearly shows a marginal increase in U concentration in the large grains of ThO_2–4%UO_2 pellet.

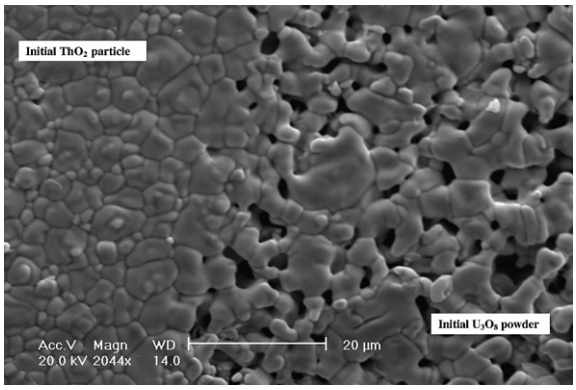

Fig. 4. Microstructure of ThO_2–20%UO_2 pellet showing duplex grain structure. Most pores are located on the initial U_3O_8 particles.

The line scan is intentionally chosen across a pore to identify the chemical composition of the pore. The counts for Th and U at pores are very low and that for oxygen is high indicating the presence of an oxide (SiO_2) which might have been picked up during the sample preparation for metallography.

The thermal diffusivity of ThO_2, ThO_2–4%UO_2 and ThO_2–20%UO_2 pellets is shown in Fig. 6 as a function of temperature. The corresponding thermal conductivity of the above samples is shown in Fig. 7. The observed thermal conductivity of ThO_2 is higher than those of ThO_2–4%UO_2 and ThO_2–20%UO_2 pellets, which is in good agreement with that reported in the literature [7]. The ThO_2–20%UO_2 pellet exhibited a very low thermal conductivity which is only about 20% of that for pure ThO_2. Also this

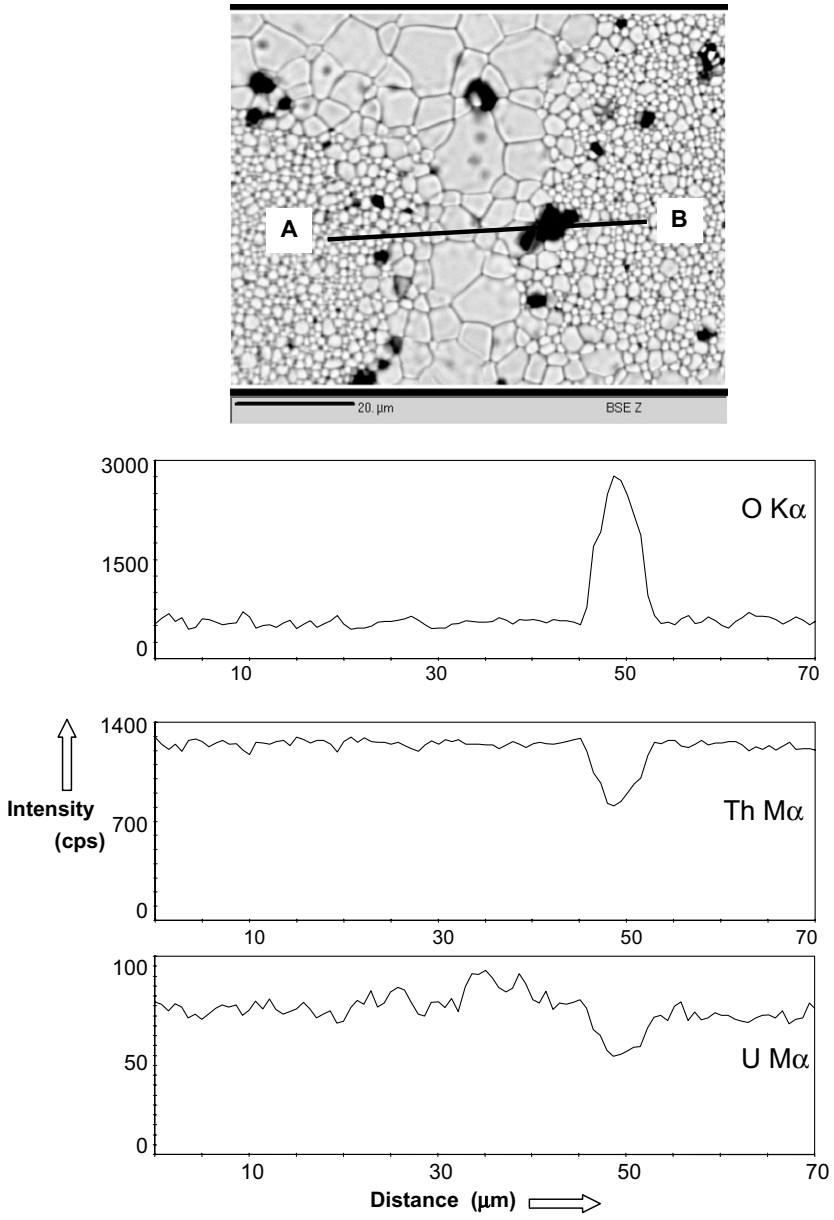

Fig. 5. X-ray line scan for Th M_α, U M_α and O K_α across the duplex grain structure for ThO_2–4%UO_2. BSE image is also shown.

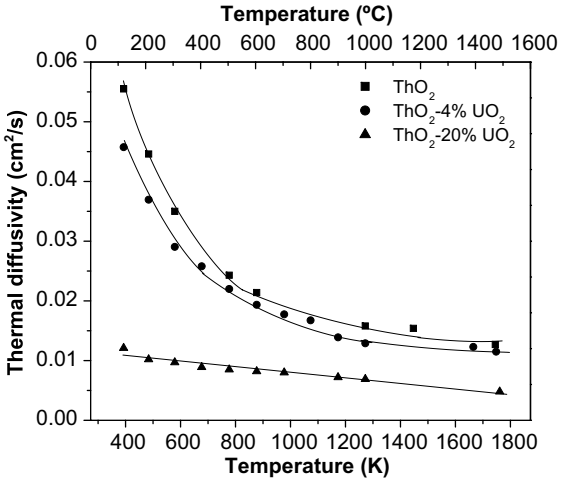

Fig. 6. Thermal diffusivity of ThO_2, ThO_2–4%UO_2 and ThO_2–20%UO_2 pellets fabricated by CAP process plotted against temperature.

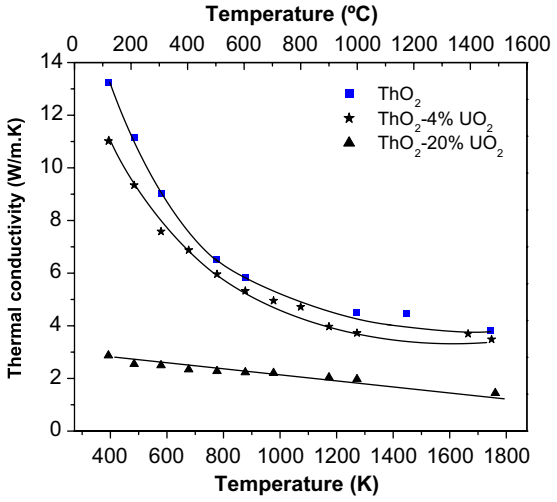

Fig. 7. Thermal conductivity of ThO_2, ThO_2–4%UO_2 and ThO_2–20%UO_2 pellets as a function of temperature.

pellet showed a very small decrease in thermal conductivity with increasing temperature.

In general, phonon–phonon scattering and phonon-impurity scattering are the dominant mechanisms of the thermal conductivity in ceramics. Klemens [14] has proposed a heat conduction model in materials where the phonon–phonon (Umklapp) scattering and the phonon-impurity scattering occur simultaneously. Theoretically the phonon component the thermal conductivity λ may be written as:

$$\lambda = (A + BT)^{-1}, \tag{4}$$

where A and B are constants and T is the absolute temperature.

Thermal resistivity (R), which is the reciprocal of thermal conductivity (λ), of the above oxides can be described by the following equation:

$$R = 1/\lambda = A + BT. \tag{5}$$

The parameter A represents the influence of phonon scattering by lattice imperfections and the parameter B describes the influence of phonon–phonon scattering [7]. The influence of substituted impurities on the thermal conductivity is described by the increase of the parameter A, while parameter B remains nearly constant by substitution. The parameter A also depends on the difference in mass and radius between the substituted atom and the host atom [1,7]. The constants A and B can be obtained from the least squares fitting of the experimental data. The linear variation of resistivity for the above samples with temperature is shown in Fig. 8. It was found that the thermal resistivity of ThO_2–4%UO_2 pellet was higher than that of pure ThO_2 and that of ThO_2–20%UO_2 pellet was found to be exceedingly high. The values constants A and B for the above oxides are given in Table 2.

Fig. 9 shows the thermal expansion of ThO_2, ThO_2–4%UO_2 and ThO_2–20%UO_2 pellets in the temperature range from room temperature to 1500 °C. The expansion curves of ThO_2 and ThO_2–4%UO_2 pellets were almost the same at all temperatures but the expansion curve of ThO_2–20%UO_2 pellet was different showing larger expansion above 1000 °C. Up to 1000 °C, however, the expansion is close to that of ThO_2 and ThO_2–4%UO_2 pellets.

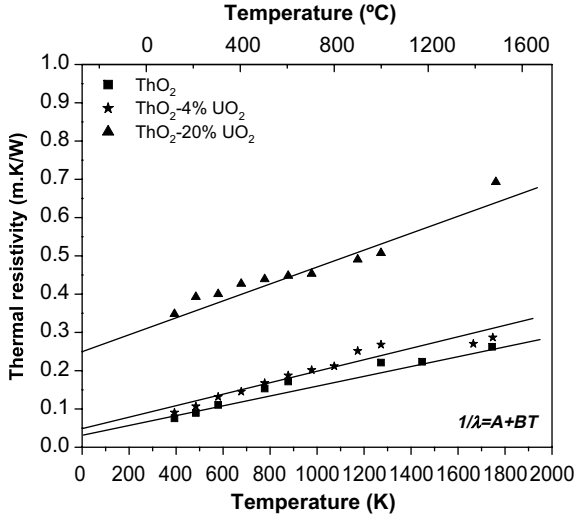

Fig. 8. Thermal resistivity of ThO_2, ThO_2–4%UO_2 and ThO_2–20%UO_2 pellets as a function of temperature. Solid lines are determined by fitting the thermal conductivity data to a relation $1/\lambda = A + BT$ using the least squares method.

Table 2
Constants A and B of the equation $1/\lambda = A + BT$ for ThO_2, ThO_2-4%UO_2 and ThO_2–20%UO_2

Sample	A, m.K/W	B, m/W
ThO_2	0.0334	1.374×10^{-4}
ThO_2–4%UO_2	0.0497	1.475×10^{-4}
ThO_2–20%UO_2	0.2516	2.359×10^{-4}

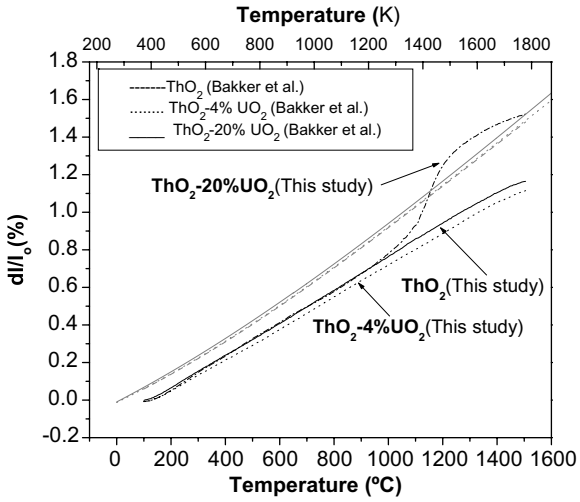

Fig. 9. Thermal expansion of ThO_2, ThO_2–4%UO_2 and ThO_2–20%UO_2 pellets made by CAP process from room temperature to 1500 °C.

The dl/l_0 versus temperature relation of ThO_2, ThO_2–4%UO_2 and ThO_2–20%UO_2 can be fitted into a third degree polynomial of the form:

$$dl/l_0 = a + bT + cT^2 + dT^3, \quad (6)$$

where dl/l_0 the expansion (in %) and T temperature in °C. The fitting is done in the temperature range of 100–1500 °C for ThO_2 and ThO_2–4%UO_2 and for ThO_2–20%UO_2 the data was fitted only in the temperature range of 100–1000 °C since above 1000 °C this sample exhibited a non-uniform expansion. The values of the constants a, b, c and d for the above compositions are given in Table 3.

The significant observations from the above study are summarized below:

1. The microstructure of the ThO_2–4%UO_2 and ThO_2–20%UO_2 pellets sintered in air showed a duplex grain structure. The grain size distribution is similar to 'rock in sand' structure.
2. The EPMA data on ThO_2–4%UO_2 and ThO_2–20%UO_2 pellets showed that the uranium concentration was marginally higher in large grained areas.
3. The thermal conductivity decreased by the addition of UO_2 to ThO_2 at any temperature.
4. The thermal expansion curve of ThO_2–20%UO_2 pellet behaves differently from those of ThO_2 and ThO_2–4%UO_2 pellets showing a much larger expansion above 1000 °C.

4. Discussion

4.1. Microstructure

The microstructure of ThO_2–UO_2 pellet prepared by CAP process showed a 'rock in sand' type structure. There were colonies of fine grains which were surrounded by large grained areas. In each of these colonies grains were randomly distributed. The size of the each fine grained colony is in range of 100–150 μm. These colonies were found to be extremely dense and some of them had no pores. These colonies represent initial ThO_2 granules, which were used for making green pellets. The identity of initial ThO_2 granules has disappeared since there was no boundary between the granules. All the granules were fused with each other (Fig. 2). In the above figure, no gap exists between the granules at any place in the pellet indicating that diffusion has occurred between them. It is true that the two regions can be distinctly observed in Fig. 2. But both these regions are having almost the same chemical composition. Nowhere in the pellet, were these granules found to be delineated. This fact suggests that diffusion has occurred between ThO_2 and UO_2. It is not possible to form a solid solution between ThO_2 and U_3O_8 since U_3O_8 does not have any solubility in ThO_2 [15]. Therefore, the U_3O_8 coating on each granule is assumed to have been decomposed to UO_{2+x} during sintering and diffused to ThO_2 matrix forming solid solution [16]. This was confirmed by EPMA.

As mentioned earlier, the grain size in the colonies was of very fine (1.7 μm). In the initial U_3O_8 for coating, grains were substantially bigger. This can be explained by considering the defect structure. ThO_2 is the only stable oxide in the Th–O system in the condensed phase and it has very little non-stoichiometry compared to UO_2 [6]. Hence the defects in pure ThO_2 are comparatively less. Since the grain growth is a diffusion related phenomenon, it depends upon the defect concentration like O_2 interstitials or metal vacancies. Therefore the grain growth is not enhanced inside the colonies. Also the temperature of the sintering ($\sim 0.45T_m$, where T_m is the melting point in K) is comparatively less. Since grain growth is diffusion controlled process, temperature of the sintering is important. Generally, diffusion processes are more prominent at temperatures $>0.5T_m$. Since the temperature of the sintering used in this study was $<0.5T_m$, this may be a factor responsible for the lower grain sizes. These two factors resulted in developing small grains in the initial ThO_2 colonies.

Table 3
Constants a, b, c and d of Eq. (6) for ThO_2, ThO_2–4%UO_2 and ThO_2–20%UO_2 pellets

Composition	a	b	c	d
ThO_2	−0.0791	6.947×10^{-4}	2.630×10^{-7}	-1.120×10^{-10}
ThO_2–4%UO_2	−0.0891	6.671×10^{-4}	2.395×10^{-7}	-9.728×10^{-11}
ThO_2–20%UO_2	−0.1259	9.611×10^{-4}	-1.927×10^{-7}	1.267×10^{-10}

On the other hand UO_2 exhibits a wide range of non-stoichiometry at elevated temperatures. This range extends from $UO_{1.65}$ to $UO_{2.25}$ at 2500 °C [17,18]. The significance of U_3O_8 addition for enhancing sintering in ThO_2, has been discussed by Kutty et al. [16]. Thermogravimetric studies carried out in air on ThO_2–2%U_3O_8 granules indicate that U_3O_8 has not been reduced to stoichiometric UO_2 even at 1500 °C. This suggests that U_3O_8 present in the green compacts will exist as UO_{2+x} at sintering temperature. Since the diffusion coefficient of U, D^U, is proportional the square of the oxygen excess (x^2) in the lattice, sintering as well as grain growth is enhanced thus resulting in bigger grains.

The basic requirements for the high performance of the fuel are [19]:

(a) 'Soft pellets' – To reduce pellet clad mechanical interaction (PCMI).
(b) Large grain size – To reduce fission gas release (FGR).

The strength of the pellet at room temperature is related to grain size by the Hall–Petch relation. Accordingly, the smaller grain sized pellets will have higher strength. But at high temperature (above equicohesive temperature) the grain boundaries become weaker than grain matrix. Since the pellets of smaller grain size have wider grain boundary areas, these pellets become softer than pellets with larger grain size. Also as the grain size decreases, the creep rate of the fuel increases. Therefore, pellets with smaller grain size have higher creep rate and better plasticity at high temperatures. These pellets will reduce the PCMI.

On the other hand, the pellets with larger grain size are beneficial to reduce the fission gas release. In developing thermal reactor fuels for high burn-up, this factor should be taken into account.

The fraction of small grained area to large grained area in ThO_2–4%UO_2 pellet obtained using CAP process is about 2:1. This fraction can be varied by varying the size of the initial ThO_2 agglomerates. The smaller agglomerate size will lead to give less volume fraction of fine grained areas.

4.2. Uranium distribution

The distribution of uranium in ThO_2–4%UO_2 and ThO_2–20%UO_2 pellets was evaluated by EPMA (Fig. 5). Both line scanning and area scanning have been carried out. The line scanning of two separate colonies of fine grains revealed that uranium has diffused to the ThO_2 granules and vice versa. Semi-quantitative analysis on the large grains (uranium rich) and also on the small grains (thorium rich) is shown in Table 4. It is seen from the table that the uranium concentration on large grains is slightly higher than that in smaller grains. Also the composition of the large grains indicates that the concentration of uranium in these grains is substantially lower than that of the starting material. This confirms that an interdiffusion has occurred between ThO_2 and UO_2 along the interface.

Table 4
Atom distribution in coarse grains and fine grains for ThO_2–4%UO_2 pellet determined by EPMA

Element	Fine grains Wt%	Coarse grains Wt %
Th	84.770	84.236
U	3.120	3.656
O	12.110	12.108

In summary, ThO_2–UO_2 fuels made by CAP process have the benefits of both small and large grains. The microstructure of comparatively fertile rich (Th) region has small grain size as indicated. Hence this region will show relatively high plasticity at high temperatures. On the other hand, the fissile rich region has larger grain size which will be of help in reducing the fission gas release. Since more fission is likely to occur in this region, more fission gas is expected to generate here. Therefore the large grains in this region can be used as storage for the fission gases. Hence we can conclude that the fuel made by CAP process has properties to reduce the fission gas release and also as well to reduce PCMI. Hence this unique microstructure will be useful in attaining high burn-up in thermal reactors.

4.3. Thermal conductivity

From Fig. 7, it is clear that the thermal conductivity of (Th–U)O_2 depends on UO_2 content and temperature. On addition of a small amount (4%) UO_2, the decrease in the thermal conductivity of ThO_2 is not large. But on addition of large quantities of UO_2, the decrease is significantly large.

Most authors [20–28] have reported that the thermal conductivity of $Th_{1-y}U_yO_2$ decreases on increasing the UO_2 content. An assessment of the thermal conductivity data of both irradiated and unirradiated ThO_2 and $Th_{1-y}U_yO_2$ solid solutions has been made by Berman et al. [24]. Bakker et al. [7] made an overview of the thermal conductivity measurements on $Th_{1-y}U_yO_2$ pellets ($0 < y \leqslant 0.2$). In all compounds the A parameter shows a large increase by substitution and B parameter shows a slight decrease by substitution. Bakker et al. [7] fitted the values A and B to obtain an equation that is valid for the low concentrations of uranium:

$$A = 4.195 \times 10^{-4} + 1.112y - 4.499y^2 \quad (7)$$

$$B = 2.248 \times 10^{-4} - 9.170 \times 10^{-4}y + 4.164 \times 10^{-3}y^2 \quad (8)$$

The thermal conductivity of nuclear ceramics is strongly influenced by its stoichiometry. The deviation from stoichiometry produce defects, most likely oxygen vacancies or metal interstitials in hypostoichiometric compounds and oxygen interstitials or metal vacancies in hyperstoichiometric compounds [29,30]. It is reported that there is a drastic change in the uranium vacancy concentration with O/U

ratio near the stoichiometric composition. Many reports are available on the effect of stoichiometry on the thermal conductivity of UO_2 and (U–Pu)O_2 samples [1,7]. This behavior is expected since introduction of point defects such as vacancies or interstitials into the oxygen ion sublattice or substitution of Th for U on the cation sublattice provides additional centers from which phonon scattering occurs. The coefficient A depends primarily on the O/M ratio and only very weakly on the uranium content [1].

The thermal conductivity of ThO_2–4%UO_2 was found to be very close to the expected value. But the thermal conductivity of ThO_2–20%UO_2 was found to be unusually low. In fact the value is smaller than that of pure UO_2. The decrease in thermal conductivity can be attributed to the O/M ratio and microstructure. The values of A and B of Bakker et al. [7] for stoichiometric solid solutions using Eqs. (7) and (8) for $y = 0.04$ and $y = 0.20$ have been calculated. The values of A for ThO_2–4%UO_2 and ThO_2–20%UO_2 pellets are 0.0377and 0.04285 mK/W, respectively. The values of B for the above compositions are 1.947×10^{-4} and 2.2079×10^{-4} m/W, respectively. On comparing these values with the values obtained in this study (Table 2), it can be seen that the value of A obtained in this study for ThO_2–4%UO_2 composition was only marginally higher but that for ThO_2–20%UO_2 was exceedingly high. The parameter A represents the influence of phonon scattering by lattice imperfections. Since the ThO_2–20%UO_2 composition has a higher O/M ratio, it resulted in the creation of large amount of point defects which has caused for the low thermal conductivity values.

The O/M ratio of ThO_2–20%UO_2 pellet was found to be high (2.07). At such high O/M, many of the U^{4+} ions will be existing as U^{5+} and U^{6+} ions. The major defects in hyperstoichiometric oxides are oxygen interstitials. The creation of defects in the lattice will lead to the enhanced phonon scattering, which results in lowering of thermal conductivity values. The microstructure of ThO_2–20%UO_2 was found to be different from that of pure ThO_2. The non-uniform microstructure resulted further reduction in thermal conductivity values.

From Table 2, it can be seen that the value of the constant A of equation increases with increase in UO_2 content. But for the ThO_2–20%UO_2 pellet the A value is considerably higher than that predicted by Eq. (7). The analysis of the lattice defect thermal resistivity and the evaluation of phonon scattering by the various defect scattering centres in pure and mixed actinide oxides have been carried out by several authors [1,20]. According to Pillai and Raj [21], the change of A value can be represented as a function of difference of mass and size of U and Th atoms and also charge difference in uranium.

The mass difference between Th and U atoms is less than 3%, and hence its contribution to thermal resistivity can be neglected. The sizes of U^{4+} and Th^{4+} ions are 0.097 and 0.100 nm, respectively. Therefore, the difference between their sizes is not appreciable and hence its contribution to thermal resistivity may also be neglected. The charge of the uranium ion depends on the O/M ratio of the pellet. This means that at higher O/M, some of U^{+4} ions are converted to U^{+5} or U^{+6} ions. Since the O/M ratio of ThO_2–20%UO_2 pellet is considerably deviated from stoichiometry, which in turn results in generation of large amounts of defects. Also the density of this pellet is the lowest. Therefore, the thermal conductivity of the ThO_2–20%UO_2 pellet was probably depressed to a low value.

4.4. Thermal expansion

Thermal expansion behaviour of ThO_2–20%UO_2 pellet was found to be different from that of ThO_2 and ThO_2–4%UO_2 pellets. For the above pellet, a non-uniform expansion was observed in the temperature range of 1000–1500 °C. This behaviour may be correlated to the high O/M ratio of the sample, i.e. O/M = 2.07. It has been reported that UO_{2+x} loses oxygen in Ar at high temperatures and tends to become stoichiometric [16]. This means that some of the U^{+6}/U^{+5} ions are getting converted to U^{+5}/U^{+4} ions [31–33]. Since ionic radii of U^{+4} (0.097 nm) and U^{+5} (0.087 nm) are bigger than that of U^{+6} (0.083 nm), the lattice expands. In short, (Th,U)O_{2+x} starts to lose oxygen above 1000 °C with lattice expansion. Below 1000 °C, the expansion behaviour was similar to that of the other two samples. This is because (Th,U)O_{2+x} loses oxygen only above 1000 °C.

The experimental values of thermal expansion for ThO_2 of the present study are compared with those of Bakker et al. [7] as shown in Fig. 9. It can be seen that the curves are parallel up to 1000 °C and then they are diverging with increase in temperature. These two curves are expected to be in good agreement since ThO_2 is a perfect stoichiometric compound. The difference for this behaviour may be attributed to the impurity contents of the starting materials. The total impurity contents of the starting ThO_2 and U_3O_8 powders used in this study are <1200 and <800 ppm, respectively (part 1, Table 1). No information on impurity for the sample used by Bakker et al. [7] is given. The expansion curves of ThO_2–4%UO_2 and ThO_2–20%UO_2 pellets of Bakker et al. [7] have also shown in Fig. 9. A similar trend was noticed on comparing them with experimental results obtained in this study for ThO_2–4%UO_2 and ThO_2–20%UO_2 pellets.

The coefficients of thermal expansion for ThO_2 and ThO_2–4%UO_2 pellets in the temperature range 200–1400 °C were found to be 8.62×10^{-6} and 8.39×10^{-6} K^{-1}, respectively. The CTE value of ThO_2–20%UO_2 pellet measured in the temperature range 200–1000 °C was found to be 9.16×10^{-6} K^{-1}. A number of authors [34–38] have measured CTE of $Th_{1-y}U_yO_2$ for a wide range of compositions. It has been found that CTE's of $Th_{1-y}U_yO_2$ lie between those of ThO_2 and UO_2, within experimental accuracy. Bakker et al. [7] have reviewed the thermal expansion behaviour of ThO_2–UO_2 system and recommended a linear decrease in the values of CTE with increase in ThO_2 concentration. The lattice parameter

for (Th,U)O_2 solid solution at room temperature decreases linearly with increase in UO_2 contents. A linear decrease in lattice parameter also exists at high temperatures [39]. Therefore a linear decrease in CTE is expected with increase in ThO_2 content. The coefficient of thermal expansion for ThO_2 obtained in this study was found to be marginally higher than that for ThO_2–4%UO_2 composition. This is contrary to the expectation, which may be attributed to the presence of duplex grain structure in ThO_2–4%UO_2. Xu et al. [40] have reported the effect of interfaces on expansion They have reported that CTE of the composite decreases with increase in volume fraction of the interfacial zone. The duplex structure in ThO_2–4%UO_2 consists of more grain boundary area and high percentage of interfaces and therefore might have caused the lower CTE values.

In summary, the CAP process can be used for manufacturing high quality ThO_2–4%UO_2 pellets. But the process may not be suitable for making ThO_2–UO_2 pellets having high uranium content such as ThO_2–20%UO_2 since it yields pellets of low density having a very low thermal conductivity values. The microstructure of the above pellet was found to be highly non-uniform with most of the pores being located on the initial U_3O_8 for coating. The above process is highly suitable for making ThO_2–UO_2 pellets having low uranium contents.

5. Conclusions

ThO_2, ThO_2–4%UO_2 and ThO_2–20%UO_2 pellets have been fabricated by CAP route using ThO_2 and U_3O_8 powders as the starting materials. The sintered pellets were characterized in terms of microstructure, uranium distribution, thermal conductivity and thermal expansion and the following conclusions were drawn:

(a) The microstructure of ThO_2–4%UO_2 and ThO_2–20%UO_2 pellets showed 'rock in sand' structure with small grains in the center of granules and large grains along the periphery. However, no delineation of granules could be found.
(b) The EPMA data confirm that uranium concentration was slightly higher in large grained areas.
(c) Thermal conductivity of sintered ThO_2 decreased by the addition of UO_2 at any temperature studied. By the addition of 4%UO_2 to ThO_2, the thermal conductivity has decreased only marginally. But by the addition of 20%UO_2, thermal conductivity has been drastically reduced.
(d) The decrease in thermal conductivity of ThO_2–20%UO_2 pellet can be attributed to their high O/M ratio, low density and inhomogeneous microstructures.
(e) The expansion curve of ThO_2–20%UO_2 pellet showed a non-uniform expansion which is attributed to the loss of oxygen of (Th,U)O_{2+x} above 1000 °C.

Acknowledgements

The authors are grateful to Mr D.N. Sah, Head, Post Irradiation Examination Division for his keen support during the course of this work. They are also thankful to Messers E. Ramadasan, J. Banerjee and K. Ravi for their valuable suggestions.

References

[1] D.R. Olander, Fundamental Aspects of Nuclear Reactor Fuel Elements, TID-26711-P1, US Department of Energy, 1976, p. 145.
[2] K. Maeda, K. Katsuyama, T. Asaga, J. Nucl. Mater. 346 (2005) 244.
[3] U.M. El-Saied, D.R. Olander, J. Nucl. Mater. 207 (1993) 313.
[4] J.A. Turnbull, C.A. Friskney, J. Nucl. Mater. 71 (1978) 238.
[5] K.C. Radford, J.M. Pope, J. Nucl. Mater. 116 (1983) 305.
[6] M.H. Rand, in: Thorium: Physico-chemical properties of its compounds and alloys, Atomic Energy Review, Special issue no.5, IAEA, Vienna (1975), p. 7.
[7] K. Bakker, E.H.P. Cordfunke, R.J.M. Konings, R.P.C. Schram, J. Nucl. Mater. 250 (1997) 1.
[8] S.E. Lemehov, V. Sobolev, P. Van Uffelen, J. Nucl. Mater. 320 (2003) 66.
[9] R.A. Young, J. Nucl. Mater. 87 (1979) 283.
[10] G.P. Marino, J. Nucl. Mater. 38 (1971) 178.
[11] T.R.G. Kutty, C. Ganguly, D.H. Sastry, J. Nucl. Mater. 226 (1995) 197.
[12] L.M. Clark, R.E. Taylor, J. Appl. Phys. 46 (2) (1975) 714.
[13] J.K. Fink, J. Nucl. Mater. 279 (2000) 1.
[14] P.G. Klemens, High Temp. High Press. 17 (1985) 41.
[15] F. Hund, G. Niessen, Z. Elektrochem. 56 (1952) 972.
[16] T.R.G. Kutty, P.V. Hegde, K.B. Khan, T. Jarvis, A.K. Sengupta, S. Majumdar, H.S. Kamath, J. Nucl. Mater. 226 (2004) 197.
[17] Hj. Matzke, J. Chem. Soc., Faraday Trans. 86 (1990) 1243.
[18] J. Belle, B. Lustman, in: Properties of UO_2, Fuel Elements Conference, Paris, TID-7546, 1958, p. 442.
[19] H.S. Kamath, in: 14th Annual Conference of Indian Nuclear Society, 17–19 December 2003, IGCAR, Kalpakkam.
[20] M.S. Kazimi, K.R. Czerwinski, M.J. Driscoll, P. Hejzlar, J.E. Meyer, On the Use of Thorium in Light Water Reactors, MIT-NFC-TR-016, April 1999.
[21] C.G.S. Pillai, P. Raj, J. Nucl. Mater. 277 (2000) 116.
[22] J.R. Macewan, R.L. Stoute, J. Am. Ceram. Soc. 52 (1969) 160.
[23] I.S. Kurina, L.S. Gudkov, V.N. Rumyantsev, Atomic Energy 92 (2002) 461.
[24] R.M. Berman, T.S. Tully, J. Belle, I. Goldberg, in: The thermal conductivity of polycrystalline thoria and thoria–urania solid solution (LMWR Development Program) Westinghouse Report WAPD-TM-908, 1972.
[25] W.D. Kingery, J. Am. Ceram. Soc. 42 (1959) 617.
[26] M. Murabayashi, S. Namba, Y. Takashi, J. Nucl. Sci. Technol. 6 (1969) 128.
[27] C. Ferro, C. Patirno, C. Piconi, J. Nucl. Mater. 43 (1972) 273.
[28] J.P. Moore, B.S. Graves, T.G. Kollic, D.I. McElroy, Oak Ridge National Laboratory Report ORNL-4121, 1967.
[29] C.R.A. Catlow, J. Chem. Soc., Faraday Trans. 2 (1987) 1065.
[30] Hj. Matzke, in: T. Sorensen (Ed.), Non-stoichiometric Oxides, Academic Press, New York, 1981, p. 156.
[31] W.I. Stuart, R.B. Adams, J. Nucl. Mater. 58 (1975) 201.
[32] K.T. Harrison, C. Padgett, K.T. Scott, J. Nucl. Mater. 23 (1967) 121.
[33] Thermodynamic and Transport Properties of Uranium Dioxide and Related Phases, Technical Reports Series No. 39, IAEA, Vienna, 1965, p. 51.
[34] P. Rodriguez, C.V. Sundaram, J. Nucl. Mater. 100 (1981) 227.
[35] C.P. Kempter, R.O. Elliot, J. Chem. Phys. 30 (1959) 1524.

[36] A.C. Momin, E.B. Mirza, M.D. Mathews, J. Nucl. Mater. 185 (1991) 308.
[37] J.R. Springer, E.A. Eldridge, M.U. Goodyear, T.R. Wright, J.F. Langedrost, Battelle Memorial Institute Report BMI-X-10210, 1967.
[38] E.D. Lynch, R.J. Beals, Argonne National Laboratory Report ANL-6677, 1962.
[39] C.A. Alexander, J.S. Ogden, G.W. Cunningham, Battelle Memorial Report BMI-1789 (1967).
[40] Z.R. Xu, K.K. Chawla, R. Mitra, M.F. Fine, Scripta Metall. Mater. 31 (1994) 1525.